



Sorption of Zn(II) ion onto the surface of activated carbon derived from eucalyptus bark saw dust from industrial wastewater: isotherm, kinetics, mechanistic modeling, and thermodynamics

Vishal Mishra*, Chandrajit B. Majumder, Vijay K. Agarwal

Department of Chemical Engineering, Indian Institute of Technology, Roorkee 247667, India
Tel. +91 9415962309; email: vishal.biochemical@gmail.com

Received 24 November 2011; Accepted 15 February 2012

ABSTRACT

The activated carbon was derived from base (0.2 M NaOH)-mediated activation of biomass followed by thermal treatment at 1,123 K. The utmost metal ion uptake capacity and sorption percentage of activated carbon derived from eucalyptus biomass were 1.42 mmol g^{-1} and 93.42%, respectively. Freundlich isotherm model proved to be superior with higher linear correlation coefficient $R^2 = 0.96\text{--}0.98$. Similarly, it was observed that pseudo-second-order reaction model with lower χ^2 (0.002703–0.009351) and sum of square errors (0.0001–0.0144) value together with higher R^2 (0.98–0.99) ruled in all the possibilities of sorption of Zn(II) ion on activated carbon surface as chemisorption. Bangham's model ($R^2 = 0.93\text{--}0.95$) applicability in the present investigation demarcated the fact that the main rate-controlling step in the sorption of Zn(II) ions on activated carbon surface was film diffusion rather than intraparticle diffusion. The results of diffusivity coefficients ($D_f = 7.16 \times 10^{-6} \text{ cm}^2 \text{ s}^{-1}$) reproduced the analogous viewpoint that film diffusion is quite a dominant step in the biosorption of Zn(II). ΔG , ΔH , and ΔS values obtained through the thermodynamic study of Zn(II) biosorption system were $-9798 \text{ kJ mol}^{-1}$, $-34.74 \text{ kJ mol}^{-1}$, and $-107.63 \text{ kJ mol}^{-1} \text{ K}^{-1}$, respectively.

Keywords: Biosorption; Zn(II) ion; Pseudo-second-order model; Film diffusion; Diffusivity coefficient

1. Introduction

The tremendous development of industrialization and civilization has given a thrust to heavy metal pollution in aqueous environment [1,2]. The heavy metals are very toxic, nonbiodegradable, and have very adverse effect on human health [3–7]. Zinc is one of the elements of the heavy metal series. The main sources of zinc pollution in aqueous solutions are metallurgical plants, galvanizing units, paint and pigment industries, alloy manufacturing units, metal finishing

operations, copper smelting plants, and acids mine drainage [8]. The limit of zinc that gets discharged from different industries to surface water reservoir ranges between 0.14 and 130 mg l^{-1} [9–13]. The permissible limit of zinc exposure defined by US Environmental Protection Agency, World Health Organization, Canadian Water Guidelines, and Minimal National Standards (Government of India) is 5 mg l^{-1} [14–16]. Earlier, it was speculated that excessive exposure of zinc results only in gastrointestinal system disorder, but the latest research suggests that zinc toxicity is also involved in renal, neural, and circulatory system disruption in vertebrates [17]. The

*Corresponding author.

presence of heavy zinc concentration in natural reservoirs results in serious threats to aquatic life [18]. Very small amount of zinc, i.e. 120 μM , has capacity to induce the micronucleus of plants, reported in case of *Vicia faba* [19]. The water frame work directive 2000/60/EC and 76/464/EEC European Union [20,21] has classified zinc as a significant element of 11 hazardous material priority list and as list two elements of dangerous substances, respectively. In the purview of the above-mentioned facts, the present investigation got motivated to remove the divalent zinc ion from the liquid phase in batch studies. Various types of conventional metal ion remediation methods have already been implemented for metal ion removal across the liquid phase viz. ion exchange, chemical precipitation, chemical oxidation and reduction, osmosis, membrane separation, electro coagulation and flocculation, reverse osmosis, and solvent extraction [22–24]. All these technologies are inefficient in removing heavy metals from liquid effluent below threshold range of 1–100 mg l^{-1} together with the generation of secondary chemical sludge, making the secondary waste disposal questionable [18,25–28]. In addition to this, affording these technologies at mass scale is not a cost-effective option for industrial units. Against the above-mentioned demerits of the conventional remedial measures, biosorption of metal ion on nonliving biomass is a very lucrative, easy, cheap, and robust process. To date, various sorts of living and nonliving biosorbents have been applied to remove zinc. Some of which are mango bark saw dust [7], pine apple fruit peel powder [7], raw eucalyptus bark sawdust [7], algae [29], fungi [30], bacteria [31], bagasse base activated carbon [15], apricot [32], olive stone [33], and esterified lemon [34]. Though these biosorbents are undoubtedly cheap, but maximum of them are of local interest. Thus their application in metal ion biosorption system makes the metal ion removal work of local interest, or in other words the biosorption process becomes non-versatile. Hence, in the light of above-mentioned statement and in search of robust and versatile biosorbent, the present investigation aimed to evaluate the biosorption potential of activated carbon derived from eucalyptus biomass (ACEUB) in accordance with Zn(II) ion sorption across liquid phase in batch studies. In the present work, the activated carbon sorption potential was evaluated as a function of isotherm, kinetic, thermodynamic parameters and physical process limits like pH, temperature and contact time. Very few researches have been done on the biosorption potential of raw and activated eucalyptus tree biomass in terms of metal ion removal [7,35–37]. Taking into account, the biological properties of eucalyptus biomass, the biomass has incredible amount of

essential aromatic oil. Usually, the oil is extracted due to its high capital value and is used as a precursor for chemical and perfume synthesis [38]. Now a days, eucalyptus essential oil is being looked as renewable source of energy [39].

2. Materials and methods

ZnCl₂ (zinc chloride anhydrous, AR grade and molecular weight 136.28 g) was dissolved in deionized water to make stock solution of 1,000 mg l^{-1} (Zn(II) ion concentration). Rest of all the batch experimental test solutions were made by diluting the stock solution up to the desired strength. The values of specific uptake capacity (q_e , mmol l^{-1}) and percentage removal were calculated by Eqs. (1) and (2), respectively [40,41].

$$q_e = C_0 - C_e \times \frac{V}{M} \quad (1)$$

$$\% \text{ biosorption} = \frac{C_0 - C_e}{C_0} \times 100 \quad (2)$$

where C_0 , C_e , V , and M are the initial concentration of Zn(II) ion, C_e is the final concentration of Zn(II) ion, V is the volume of solution (l), and M is the mass of biosorbents (g). The suitability of isotherm, kinetic, and thermodynamic models has been evaluated in terms of linear correlation coefficient, chi-square (χ^2) test, and sum of square errors (SSE). The mathematical functions used to calculate the χ^2 value and SSE function are represented in Eqs. (3) and (4).

$$\chi^2 = \sum \frac{[q_e(\text{Exp}) - q_e(\text{Th})]^2}{q_e(\text{Th})} \quad (3)$$

$$\text{SSE} = \sum_{i=1}^m [q_e(\text{Th}) - q_e(\text{Exp})]^2 \quad (4)$$

2.1. Activated carbon preparation

Eucalyptus bark was obtained from the institute campus. The bark was dried and washed three times with distilled water followed by drying in sun for two days. After drying, the dead biomass was ground in particle in ball mill and powder obtained was sieved to the particle size of 0.5 mm. The selected biosorbent particles were treated with 0.2 M NaOH (2 g/150 ml)

for 24 h at 383 ± 1 K in an oven. After the completion of reaction time, the residual carbon was washed thrice with deionized water till the pH of the residual water became neutral, i.e. 7. To fix the color of the biosorbent, the activated sample was treated with 2% formaldehyde in a ratio of 1:4 (w/v). The treated sample was washed three times with distilled water to remove the unbounded formaldehyde. The activated carbonized biomass obtained after washing was dried in oven at 378 K for 1 h. Thermal activation of carbonized material was carried out by heating the sample 1,123 K for 30 min [15].

3. Results and discussion

3.1. Optimization of pH and temperature

The pH of the biosorption system significantly influences the metal ion speciation, surface chemistry of the biosorbent surface, and adsorption of adsorbate onto adsorbent surface [42,43]. In the present investigation, a pH range of 3–7 was selected for biosorption batch test runs. The influence of pH on Zn(II) ion biosorption has been studied in Figs. 1 and 2.

It became evident from Fig. 1 that at low pH, i.e. at 2, the metal ion sorption was very low, about 23.27%. With the increase in pH from 3 to 5, metal ion sorption increased from 44.56 to 93.42%. The maximum metal ion removal (93.42%) was obtained at pH 5. In between pH 6 and 7 and above the metal ion speciation got changed from divalent zinc ion, i.e. Zn (II) ion to hydroxide complex, Zn (OH)₂ [44], resulting in the precipitation of metal ion rather than metal ion adsorption. Rocha et al. [44] reported a slight decrease in the adsorption capacity of the rice husk for metal ion sorption at a pH, initial starting pH, greater than 5. This was because of the fact that the higher pH of the system would have caused the positive charge

diminution on divalent metal ion resulting in the conversion of dominant divalent zinc ion species to hydroxide complex. In the present investigation, the sorption capacity of the ACEUB has also found to be decreased above pH 5 due to the change of metal ion speciation resulting in lower q_e and higher C_e , as can be seen from Figs. 1 and 2. At very low pH, i.e. 2, lower Zn(II) ion sorption onto the surface of activated carbon was due to the extensive and praiseworthy competition between hydrogen ion and metal ion present in the liquid phase. Additionally, the active sites present on the surface of activated carbon got protonated resulting in the diminution of negative charge density present at the biosorbent-based active sites leading to the generation of repulsive forces in between Zn(II) ion and active sites [45,46]. The increase in pH from 3 to 5 imparted an optimistic impact on Zn(II) sorption onto the activated surface biomass. The rationale behind the increment reported in Zn(II) ion adsorption/percentage removal with the increase in pH was the lowering of hydrogen ion concentration in liquid phase and positive charge density diminution present on the adsorptive active sites leading to the generation of attractive forces between metal ion and active sites [47] resulting in more possibilities of Zn(II) ion binding with ACEUB carbon particles.

The influence of pH on uptake capacity (q_e , mmol g^{-1}) and equilibrium concentration (C_e , mmol l^{-1}) of the biosorbent has been studied in Fig. 2. The pH variation in the range of 2–5 significantly affects the biosorbent uptake capacity (mmol g^{-1}) and equilibrium concentration (C_e , mmol l^{-1}). The increase in pH from 2 to 5 in the liquid phase dramatically increases the uptake capacity from 0.1 (mmol g^{-1}) to 1.42 (mmol g^{-1}) with a simultaneous decrease in equilibrium concentration from 1.4 (mmol l^{-1}) to 0.1

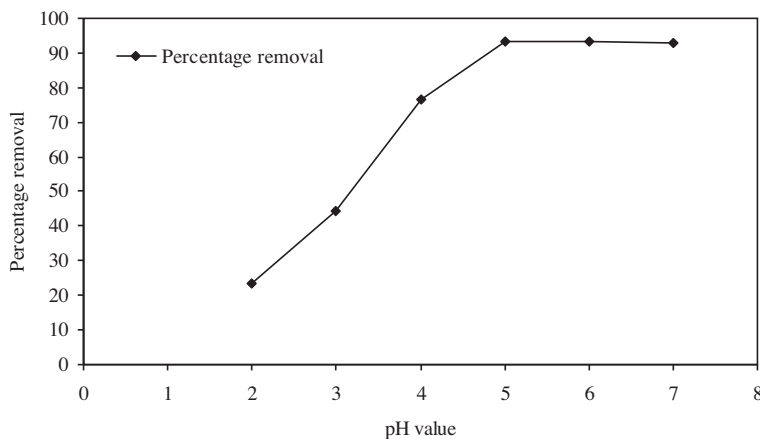


Fig. 1. Influence of pH on Zn(II) ion biosorption (at 1.52 mmol l^{-1} Zn(II) ion initial concentration, at 150 rpm, 298 ± 1 K).

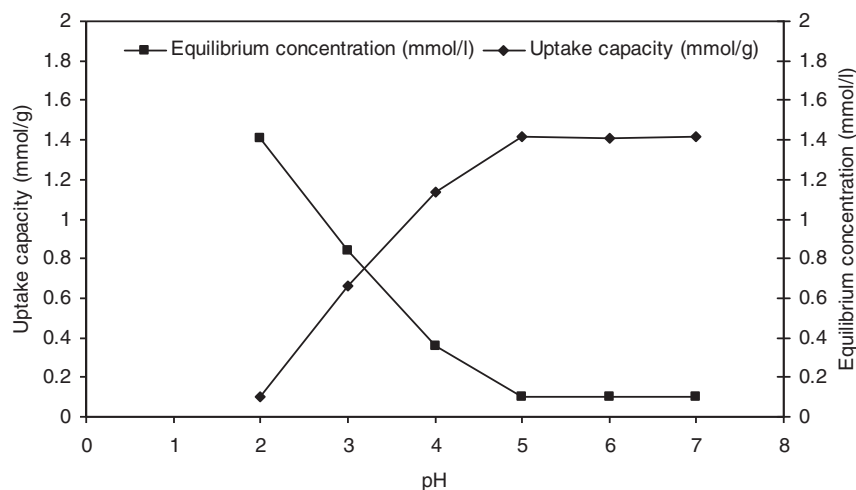


Fig. 2. Influence of pH on uptake capacity and equilibrium concentration of Zn(II) ion (at 1.52 mmol l^{-1} Zn(II) ion initial concentration, at 150 rpm, $298 \pm 1 \text{ K}$).

(mmol l^{-1}). The simultaneous decrease and increase in equilibrium concentration and uptake capacity, respectively, with simultaneous variation of pH from 2 to 5, clearly demarcated the privileged biosorption of Zn(II) ion across the liquid phase onto the surface of ACEUB at higher pH range, in present investigation. In pH range of 5–7, the sorption of Zn(II) ion got reduced to 93.06% resulting in an increase in equilibrium concentration ($0.105 \text{ mmol l}^{-1}$). Hence, in the present research work, pH 5 was considered for all other batch experiments.

The temperature of the biosorption system is another significant parameter that affects the metal ion removal or percentage sorption across liquid phase. The variation in biosorption behavior of metal ion together with adsorption active sites is usually justified in terms of exothermic and endothermic surface ligand reactions. In the present investigation three temperature gradients 298, 308, and 318 K were validated to manifest the biosorption reaction either as exothermic or endothermic reaction. The results of effect of temperature on Zn(II) ion biosorption are represented in Fig. 3.

With the increase in temperature from 298 to 318 K, a simultaneous decrease in uptake capacity (mmol g^{-1}) from 1.41 to 0.98 was reported. In addition to this, a subsequent increase in equilibrium concentration (mmol l^{-1}) of Zn(II) ion in aqueous media was also observed with an increase in temperature. The decrease in biosorptive uptake capacity (mmol g^{-1}) at higher temperature profile together with the increase in equilibrium concentration (mmol l^{-1}) of metal ion in liquid phase from 0.1 to 0.52 indicated that the Zn(II) ions sorption onto ACEUB active sites was not

temperature dependent, i.e. Zn(II) ion adsorption onto the activated carbon surface was exothermic in nature. The maximum uptake capacity of ACEUB was reported about 1.42 mmol g^{-1} at 298 K. Therefore, optimized temperature 298 K was implemented for all other batch test runs. Very conflicting results are available in the description of temperature disposition of biosorption system. Dang et al. [27] have clearly reported the ambiguity in temperature related results of metal ion sorption. The authors [27] concluded such dispraised results as an outcome of implementation of different sorts of biomasses/biosorbents collected from different geographical locations. In the present work, Zn(II) ion sorption onto ACEUB surface seemed to be an exothermic reaction. The exothermic nature of Zn(II) ion binding onto the surface of ACEUB indicated chemisorption as the preferred mode of Zn(II) adsorption onto activated carbon surface. Ifthikar et al. [18] reported the exothermic behavior of Cu(II) and Cr(III) ion on rose biomass surface. The results of previous findings [18,27] are quite consistent with the present work findings. The rationale behind the maximum metal ion uptake capacity (1.42 mmol g^{-1}) at the lowest temperature profile or gradient (298 K) was the denaturation of the active sites present on the surface of the activated biomass at higher temperatures (308 and 318 K) compared to lower temperature [18].

3.2. Optimization of adsorbate to adsorbent ratio

The availability of adsorbate (zinc) species in liquid phase significantly affects the biosorption efficiency of batch biosorption system, in terms of metal ion removal. In present investigation five different

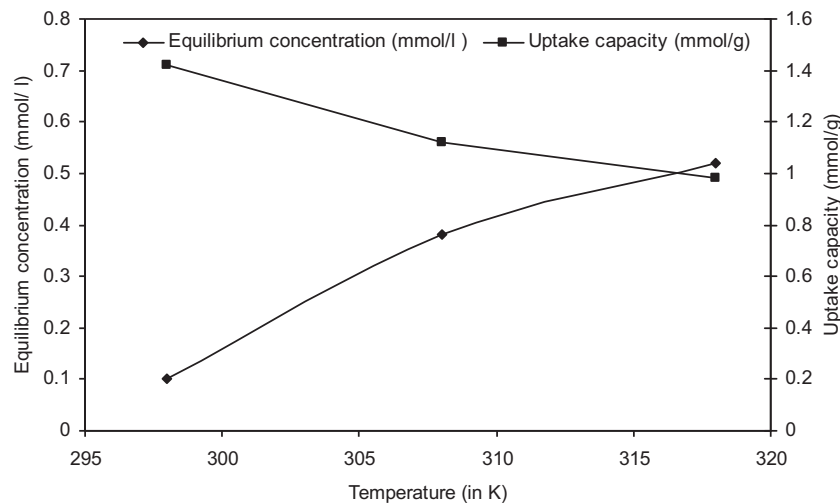


Fig. 3. Influence of temperature variation on Zn(II) ion biosorption onto the surface of ACEUB at pH 5, 150rpm, and adsorbate dose 1.52 mmol l^{-1} .

concentration ranges 0.38, 0.76, 1.15, 1.52 and 1.91 mmol l^{-1} per gram of biosorbent were used to find out the optimized adsorbate dose for ACEUB-mediated Zn(II) ion biosorption. The results of influence of adsorbate dose on Zn(II) ion biosorption are represented in Fig. 4.

Uptake capacity of ACEUB got increased from 0.36 to 1.42 mmol g^{-1} with the increase in adsorbate concentration from 0.38 to 1.52 mmol l^{-1} . But the increase in adsorbate dose above 1.52 mmol l^{-1} by 0.39 mmol l^{-1} did not significantly affect the uptake capacity of ACEUB. Additionally, the equilibrium concentration of Zn(II) ion followed a linear trend of increment in between adsorbate concentration range of $0.39\text{--}1.52 \text{ mmol l}^{-1}$, but at concentration gradient above 1.52 mmol l^{-1} , a relative but sharp increase was observed in the equilibrium concentration of metal ion. The increase in uptake capacity per unit mass of

biosorbent with the increase in zinc concentration in liquid phase was due to the tending towards the approach of saturation of adsorptive active sites, resulted concurrently in decrease in the equilibrium concentration of metal ion in aqueous medium. The removal of metal ion felt an increase up to 1.52 mmol l^{-1} concentration since the higher concentration gradient rules out all the mass transfer resistances resulting in the saturation of high energy active sites [25]. But with the saturation of active sites at higher metal ion concentration, the specific uptake capacity got stagnant or fixed leading to a sharp upsurge in equilibrium metal ion concentration, as can be seen from Fig. 4. The lowering of metal ion removal above 1.52 mmol l^{-1} was due to the saturation of higher energy active adsorptive sites resulting in the interaction of lower energy active sites with the Zn(II) ion, at upsurged concentration [48–50]. In the present investi-

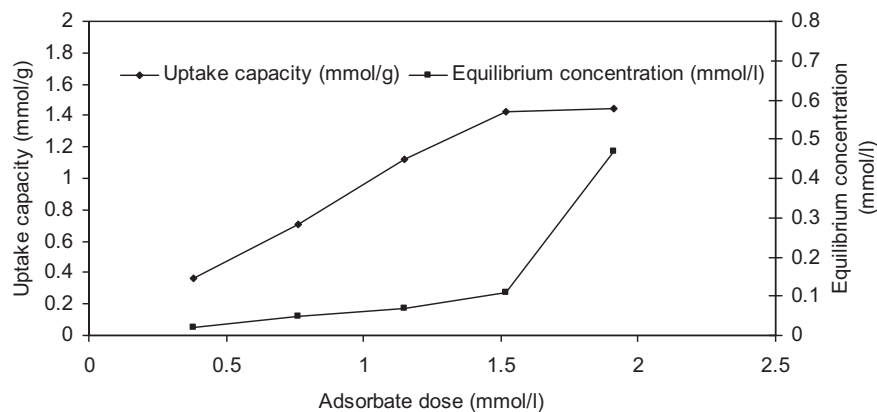


Fig. 4. Influence of adsorbate dose (mmol l^{-1}) on Zn(II) ion biosorption at pH 5, 150rpm, adsorbent dose 1 g l^{-1} , and temperature $298 \pm 1 \text{ K}$.

gation, adsorbate dose of 1.52 mmol l^{-1} was found suitable to achieve maximum efficiency of biosorbent in terms of Zn(II) biosorption across liquid phase in batch studies. Therefore, in rest of all batch experiments, optimized adsorbate concentration, i.e. 1.52 mmol l^{-1} , was allocated.

The biosorbent or biomass concentration (g l^{-1}) is also a very crucial factor that determines the sorption efficiency of biosorption system. The dose or concentration of biomass affects the number of active binding sites present on the surface of adsorbent thus affecting the metal ion uptake capacity per unit of biomass. In the present work, biomass dose in the range of $0.2\text{--}1.0 \text{ g l}^{-1}$ was applied on Zn(II) ion biosorption and its effects on Zn(II) ion removal has been studied in Fig. 5.

As can be seen from Fig. 5, with the increase in biosorbent dose from 0.2 to 1.0 g l^{-1} , the adsorption uptake capacity got decreased from 2.21 to 1.42 mmol g^{-1} together with noteworthy and linear lowering in equilibrium metal ion concentration from 1.088 to 0.11 mmol l^{-1} , in the liquid phase. The decrease in uptake capacity and equilibrium concentration of ACEUB and metal ion, respectively, with an increase in biosorbent dose was due to the increase in the number of binding sites present on the surface of ACEUB and the effective surface area of biosorbent meant for metal ion binding [21,25,28,51]. The increase in the number of binding sites and enhanced surface area provided more opportunity to Zn(II) ions to bind with activated carbon surface resulting in the lowering of uptake capacity and equilibrium concentration of metal ion leading to the attainment of maximum percentage metal ion removal across liquid phase.

3.3. Determination of contact and equilibrium time

Zn(II) ion biosorption was studied up to 150 min. The results of contact and equilibrium time determi-

nation were correlated with the percentage removal of metal ion at the onset of process followed by other differential stages at the time of biosorption reaction till the equilibrium was approached. Results of influence of contact time on Zn(II) ion biosorption are shown in Fig. 6.

The metal ion sorption was very fast for the first 31 min (30.4 min accurately), approximately, 78.4% of metal ion got removed. In the next time slot of another 2 h, the removal percentage of metal ion was relatively higher, but the rate of removal was very slow. After the fast and quick removal of metal ion in the first 31 min of the initiation of biosorption reaction, the rate of metal ion removal became slow and decreased in another 2 h of reaction time. The rapid uptake of metal ion in the first timepiece of 31 min was dedicated to the large number of high energy active vacant sites present on the surface of ACEUB due to larger surface area exposed to the metal ion [52] together with the presence of high pressure/concentration gradient of metal ions in the liquid phase. But with the passage of time, the mass transfer/pressure gradient became weakly coupled with the saturation of high energy active sites leading to the movement of adsorbate species/metal ions inside the pores of adsorbent resulting in delayed attainment of sorption equilibrium. Therefore, in all other batch experiments of isotherm and kinetic model, the contact was taken as 2.4 h. Regarding the realization of equilibrium time, the present investigation calculated the equilibrium time as a function of percentage removal, the Zn(II) ion equilibrium removal was realized in almost 2.3 h, as can be seen from Fig. 6.

3.4. Isotherm, kinetic, and thermodynamic model

Adsorption isotherm has its special importance in determining the partition of metal ion in between

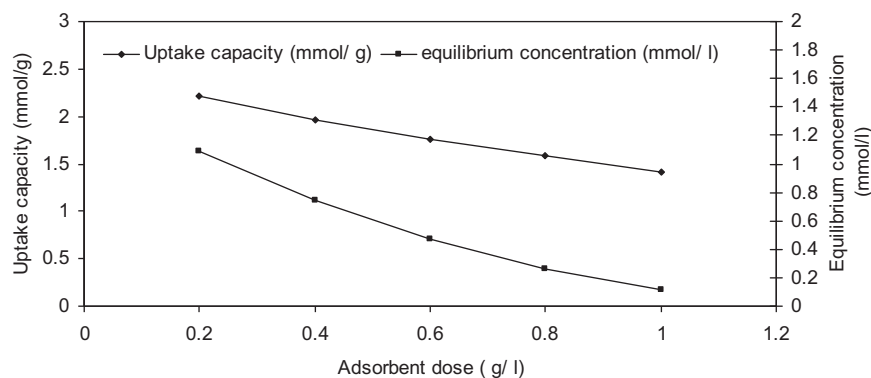


Fig. 5. Influence of adsorbent/biosorbent dose on Zn(II) ion sorption at pH 5, 150 rpm, adsorbate dose 1.52 mmol l^{-1} , and $298 \pm 1 \text{ K}$.

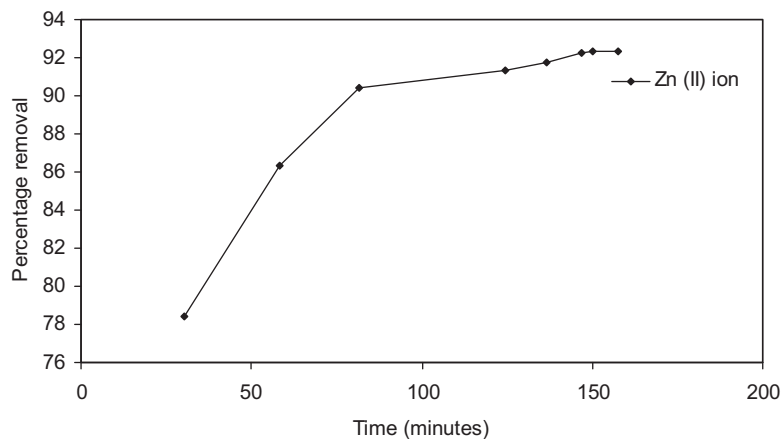


Fig. 6. Influence of contact time on Zn(II) ion sorption at pH 5, 298 ± 1 K, and 150 rpm.

solid and liquid phase at the attainment of equilibrium. The data obtained in isothermal modeling notably help in the fabrication of continuous reaction columns required in dynamic studies. The present investigation has dealt with two well-known isotherm models *viz.* Langmuir and Freundlich isotherm, and isotherms were validated to correlate the data derived at constant temperatures, at different concentration gradient of metal ion with a fixed dose of adsorbent. All the experiments were repeated thrice, all average values were kept in data cum curve fitting and statistical analysis of the data was done by linear correlation function (R^2) inbuilt function in Microsoft Excel 2003 together with the interpretation of goodness of fit in terms of chi-square (χ^2) test and SSE.

3.4.1. Langmuir isotherm

Langmuir model assumes that the surface of the biosorbent is homogeneous and all adsorptive active sites are energetically symmetrical resulting in the monolayer coverage of biosorbent [53,54]. The Langmuir isotherm has been shown in Eq. (5).

$$q_e = \frac{q_{\max} b C_e}{1 + b C_e} \quad (5)$$

where q_{\max} (mmol g^{-1}) and b (l mmol^{-1}) are maximum sorption capacity and Langmuir isotherm constant, respectively. The extrapolation of the curve between C_e/q_e and C_e yields a straight line. The straight-line equation reproduces the value of b and q_{\max} as intercept and slope of the line. The model was studied in the range of $0.38\text{--}1.52 \text{ mmol l}^{-1}$. The results of Langmuir isotherm model study are shown in Fig. 7 and Table 1.

The Langmuir isotherm model study shown in Fig. 7 and tabulated in Table 1 indicated that at all the temperature ranges, Langmuir model yielded a satisfactory explanation of Zn(II) ion biosorption onto the surface of ACEUB in terms of quite high linear correlation coefficients. The data represented in Table 1 and Fig. 7 demarcated the Zn(II) ion sorption onto the surface of ACEUB as temperature-independent reaction. A linear and steady decrease in the uptake capacity (q_e , mmol g^{-1}) was observed with temperature elevation from 298 to 318 K. Additionally, a conflicted result at 318 K was reported with higher maximum uptake capacity (1.62 mmol g^{-1}) against maximum uptake capacity observed at 308 K, about $1.53 \text{ (mmol g}^{-1})$. The contradicted results have led to the bewildering temperament of Zn(II) ion sorption onto activated carbon surface. Therefore, in the present investigation, it seems that it is better to justify the isotherm temperature dependency or independency in terms of curve's goodness of fit, i.e. linear regression coefficient (R^2) and as expected, a very satisfactory and momentous isotherm goodness of fit was obtained at two temperature gradients worth mentioning at 298 and 308 K. The increase in temperature up to 318 K yielded comparatively low model R^2 , thus justifying the temperature independency of Zn(II) sorption onto the surface of ACEUB. Further, the Langmuir isotherm suitability for Zn(II) ion sorption onto the activated carbon surface was interpreted in terms of dimensionless factor R_L (also known as separation factor). The empirical relation for the determination of separation factor has been represented in Eq. (6).

$$R_L = \left[\frac{1}{1 + b C_0} \right] \quad (6)$$

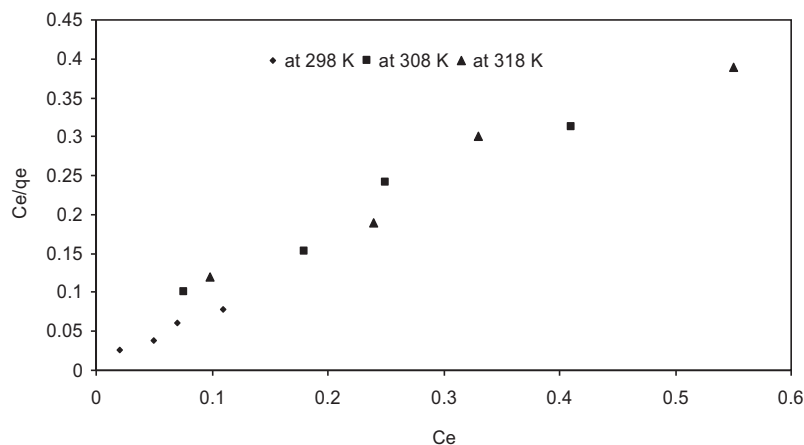


Fig. 7. Langmuir isotherm model study on Zn(II) biosorption onto the surface of ACEUB.

Values of R_L and its corresponding meaningful interpretation are as follows

R_L —value Classification of isotherm

$R_L > 1$ —Unfavorable

$R_L = 1$ —Linear

$0 < R_L < 1$ —Favorable

$R_L = 0$ —Unfavorable

The value of R_L was calculated and it was about 0.125, which gives quite satisfactory and momentous applicability of Langmuir isotherm model in the present investigation. Results of separation factor at different temperature gradients are shown in Table 1.

3.4.2. Surface area coverage

Removal of Zn(II) ion across liquid phase mediated by biosorption mechanism can also be explained in terms of surface area coverage and separation

factor. The relation required to calculate surface area coverage has been represented in Eq. (7).

$$K_L C_0 = \frac{\theta}{1 - \theta} \quad (7)$$

where K_L is same as b , i.e. Langmuir isotherm constant ($l \text{ mmol}^{-1}$) and θ correspond to the surface area coverage. Results of surface area coverage as a function of initial metal ion concentration and separation factor are shown in Fig. 8.

It became evident from Fig. 8 that with the increase in initial metal ion concentration from 0.38 to 1.52 mmol l^{-1} , a simultaneous increase in the proportion of surface area coverage is observed until a monolayer was formed over the total surface of biomass. In addition to this, relatively lower value of separation factor (R_L) was observed at higher concentration ranges relatively. A sharp and linear trend of separation factor decrement

Table 1
Langmuir and Freundlich isotherm model parameter study

Model/isotherm	Temperature (K)	q_e (mmol g^{-1})	q_{\max} (mmol g^{-1})	b ($l \text{ mmol}^{-1}$)	R^2
<i>Langmuir model</i>					
	298	1.42	1.63	4.57	0.96
	308	1.12	1.53	12.56	0.96
	318	0.98	1.62	9.87	0.95
<i>Freundlich model</i>					
			$1/n$	K_f ($l \text{ g}^{-1}$)	
	298	1.42	0.8233	8.92	0.98
	308	1.12	0.8026	2.42	0.97
	318	0.98	0.7544	1.63	0.96

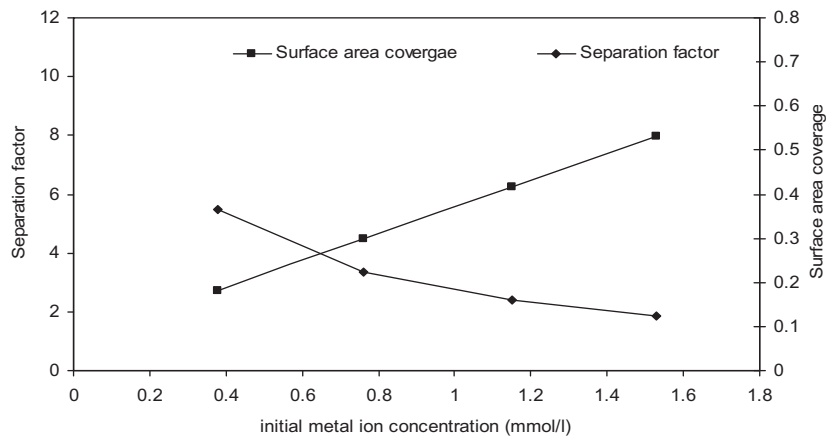


Fig. 8. Study of surface area coverage as a function of initial metal ion concentration and separation factor at 150 rpm, biomass dose 1 g l^{-1} , pH 5, and temperature 298 K.

was noticed and the fallout of separation factor was expected to be the outcome of biomass surface saturation at higher metal ion concentration level.

3.4.3. Freundlich isotherm

This isotherm model assumes the presence of heterogeneous surface on biomass surface resulting in different sorption energies and multilayer coverage of biomass surface [55]. The isotherm in its nonlinear is represented in Eq. (8) [54].

$$q_e = K_f C_e^{1/n} \quad (8)$$

K_f = Freundlich constant (l g^{-1})
 $1/n$ = affinity constant/indicator

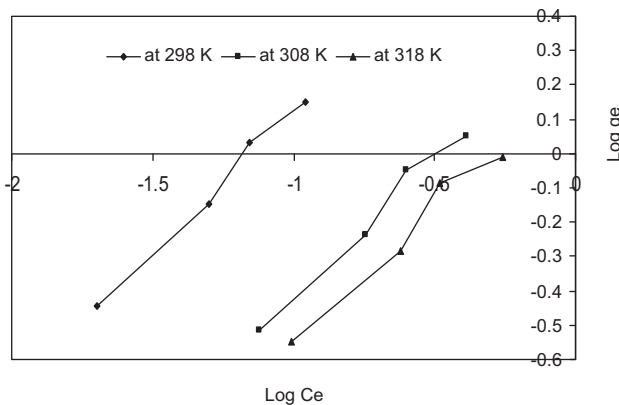


Fig. 9. Study of Freundlich isotherm model at 150 rpm, 1 g l^{-1} biosorbent dose, and at temperature range between 298 and 318 K.

The results of Freundlich isotherm study are shown in Table 1 and Fig. 9.

The comparative analysis of Langmuir isotherm against Freundlich isotherm model made a supportive indication that both the models have substantial potential to describe the Zn(II) ion binding on the surface of ACEUB. More precisely, Freundlich model has a prospective of biosorption of Zn(II) ion across liquid phase. It can be easily seen from Table 1 that in case of Freundlich isotherm, the linear regression coefficient R^2 value is quite higher, ranging between 0.98 and 0.96 against Langmuir isotherm linear regression coefficients that are ranging between 0.96 and 0.95. The values of $1/n$ are quite below the unity, i.e. $1/n < 1$ at all the temperature ranges, which further proves the favorable adsorption in terms of Freundlich adsorption [56]. Consequently, in the present work, it was concluded that Langmuir and Freundlich isotherm both have sufficient throughput to describe the adsorption of Zn(II) ion on the surface of ACEUB at all the ranges of temperature, ranging in between 298 and 318 K. In both the isotherms, Freundlich model was found to be superior to Langmuir model at all the temperature ranges together with permissible value of affinity constant, i.e. $1/n$ below unity.

3.5. Kinetic modeling

Kinetic or dynamic modeling is a very imperative concept to elucidate the rate and mechanism of reaction in conjunction with the determination of rate-controlling step [57]. On the other hand, the study of dynamic studies becomes praiseworthy in terms of continuous reaction column design and fabrication [58]. The present investigation has undertaken four well-known kinetic models viz. pseudo-first-order,

pseudo-second-order, intraparticle diffusion, and Bangham's model to chalk out the exact mode and mechanism of Zn(II) ion sorption onto the activated carbon surface.

Considering the reversible binding of Zn(II) ion with the active sites present on the surface of ACEUB and the rate of adsorption directly proportional to the number of vacant binding sites, pseudo-first-order model got applicable and is represented in Eqs. (10) and (11). Eq. (9) represents the schematic diagram of reversible Zn(II) ion binding with adsorptive active sites.



where B is an active adsorptive site.

Eq. (10) represents the differential form of pseudo-first-order model

$$\frac{dq_t}{dt} = K_1(q_e - q_t) \quad (10)$$

where q_t is the uptake of metal ion per unit of adsorbent mass at time t and K_1 is the reaction constant (min^{-1}). On the integration of Eq. (10) at boundary conditions, i.e. at $t=0$ to $t=t$ and from $q=0$ to $q=q_t$ at time t , Eq. (11) is obtained.

$$\text{Log}(q_e - q) = \text{Log}q_e - K_1t \quad (11)$$

Eq. (10) represents the straight-line equation of integrated pseudo-first-order model. The extrapolation of curve between $\text{log}(q_e - q_t)$ and t yields the value of K_1 (min^{-1}) as slope of the curve.

Pseudo-second-order model assumes the chemisorption mode of adsorbate binding with adsorbent particle [59]. Eqs. (12) and (13) represent the differential and integral form of pseudo-second-order model

$$\frac{dq_t}{dt} = K_2(q - q_t)^2 \quad (12)$$

Integrating Eq. (12) at boundary conditions reproduces Eq. (13)

$$\frac{t}{q_t} = \frac{1}{K_2q_e^2} + \frac{t}{q_e} \quad (13)$$

Eq. (14) represents the straight-line equation of pseudo-second-order model and the extrapolation of plot between t/q_t and t yields the value of theoretical q_e and K_2 (reaction constant, $\text{g mg}^{-1} \text{min}^{-1}$). The results of pseudo-first- and pseudo-second-order model are shown in Table 2 and Figs. 10 and 11.

It became evident from Figs. 10, 11, and Table 2 that pseudo-second-order model undoubtedly provides a better understanding of the sorption mechanism of Zn(II) ion. Moreover, the value of experimental uptake capacity q_e (mmol g^{-1}) was found in agreement with the theoretical uptake capacity reported through the pseudo-second-order kinetic model. The initial sorption rate h ($\text{mmol}^{-1} \text{g}^{-1} \text{min}^{-1}$) in conjugation with rate constant (K_2 , $\text{g mmol}^{-1} \text{min}^{-1}$) was found to follow almost linear trend with the adsorbate dose increment, significantly approving the capability of pseudo-second-order model to interpret the metal ion sorption onto the active sites as chemisorption. The deep insight of metal ion binding onto ACEUB surface was deciphered by extrapolating the logarithmic plots in between initial concentration and initial sorption rate h and model constant K_2 . The results of initial adsorbate concentration influence on initial sorption rate and rate constant are given in Fig. 12 and Eqs. (14) and (15).

$$h = 0.5497C_0 - 1.0021 \quad R^2 = 0.73 \quad (14)$$

$$K_2 = -0.592C_0 + 0.138 \quad R^2 = 0.95 \quad (15)$$

The scrutiny of Fig. 12 chalked out the verity that initial sorption rate points with upsurged concentration gradient of adsorbate yielded a linear and increasing trend line contrary to model reaction constant K_2 . Basha et al. [60] reported a similar type of observation for Hg(II) ion sorption onto *Carica papaya*-based sorbent. On the contrary, Kumar et al. [61] and Ho and Mc Kay [62] observed the decrease in both the trend lines reproduced from the initial sorption rate and model reaction constant for dye particle adsorption onto the surface of fly ash and peat surface, accordingly. The conduct of all the rate derivatives of pseudo-second-order model at various initial concentrations of Zn(II) ion was consistent with the results obtained in the biosorption of Cr(VI) removal onto the surface of pomegranate husk [63].

3.6. Mechanistic modeling

In the present investigation, two well-known mechanistic models worth mentioning intraparticle or Weber Morris and Bangham's model have been studied to uncover the mechanism of Zn(II) ion adsorption/binding onto ACEUB surface. Eq. (16) represents the linearized form of intraparticle model.

$$q_e = K_{id}t^{0.5} + I \quad (16)$$

K_{id} = Intraparticle diffusion constant ($\text{mmol g}^{-1}\text{min}^{-0.5}$).

Results of intraparticle model are represented in Table 3 and Fig. 13.

The momentous convective mass transfer reaction in cylindrical coordinates across liquid phase through the mesoporous surface of activated nonliving biomass surface is a three-step-mediated process consisting of (i) adsorbate or metal ions shipping from bulk liquid phase including boundary layer surrounding the adsorbent/biosorbent particle to the surface of adsorbent, known as film or bulk diffusion, (ii) sorption of adsorbate/metal ions onto the surface of biomass, this step is quite fast, and (iii) movement of metal ions inside the pores of adsorbate particle across the liquid-filled inside pores or by solid-phase diffusion mechanism [64]. Kinetics of metal ion sorption onto the surface of biomass can be regulated by any of the above-mentioned steps singly or in combination. Fig. 13 represents, the multilinear temperament of intraparticle model. Such types of curves have already been reported in previous research findings [65,66]. The multilinear curve of the intraparticle model with intercept I established the aspect that both intraparticle diffusion of metal ion through the mesoporous openings filled with liquid and film/external mass transfer across the thickness of boundary layer were the rate-determining steps in the biosorption of Zn(II) kinetics on the surface of ACEUB. The value of intercept I obtained through the model yields the value of thickness of boundary layer of liquid surrounding the biomass particle. The study of the individual data points obtained in Fig. 13 and Table 3 indicates that intraparticle mechanistic model was not suitable to lucratively and proficiently describe the sorption of Zn(II) ion onto the surface of ACEUB in terms of lower regression coefficient, ranging between 0.80 and 0.85. Therefore, to find out the best possible mechanism of Zn(II) ion, which would have rolled as

rate-limiting step, another model known as Bangham's model has been implemented. The linear logarithmic Bangham's rate model is represented in Eq. (17).

$$\text{Log} \left[\log \left\{ \frac{C_0}{C_0 - q_m} \right\} \right] = \log \left\{ \frac{K_0 m}{2.303V} \right\} + \alpha \log(t) \quad (17)$$

where q is the uptake capacity (mmol l^{-1}), m is the mass of biosorbent (g), and $\alpha > 1$ and K_0 are the model constants. The results of the concerned model are represented in Table 3 and Fig. 14. The goodness of fit of curve for Bangham's model was correlated in terms of linear regression coefficient (R^2).

The considerable dominance of Bangham's model over intraparticle model could be justified from Table 3. The significant regression coefficients obtained for Zn(II) ion sorption onto the surface of activated carbon across the liquid phase in terms of Bangham's model rejuvenated the information that film diffusion has played very noteworthy part in determining the rate of Zn(II) ion mass transfer onto the surface and inside the biomass particle.

3.7. Diffusivity coefficient validation

However, the Bangham's model was proved superior to intraparticle model in terms of higher linear regression coefficient (R^2), but itself the value of linear regression coefficient was not satisfactory to describe metal ion binding mechanistically onto the biomass surface. Therefore, it becomes difficult to rule out the insignificant step in Zn(II) ion sorption cum biosorption onto the surface of ACEUB as not be mentioned as rate-limiting or determining step. For this reason, the diffusivity coefficients were tested, in particular film (D_f) and pore diffusion (D_p) were experienced.

Table 2

Study of pseudo-first- and pseudo-second-order model in the concentration range of 0.38–1.52 mmol l^{-1} , pH 5, 150 rpm and at 298 K

Zn(II) concentration (mmol l^{-1})	Pseudo-first-order model						Pseudo-second-order model					
	q_e^{exp} (mmol g^{-1})	q_e^{cal} (mmol g^{-1})	$K_1 \times 10^{-2}$ (min^{-1})	R^2	SSE	χ^2	q_e^{cal} (mmol g^{-1})	K_2 ($\text{g mmol}^{-1} \text{min}^{-1}$)	h ($\text{mmol}^{-1} \text{g}^{-1} \text{min}^{-1}$)	R^2	SSE	χ^2
0.38	0.36	4.033	1.44	0.90	13.49	3.34	0.37	0.39	0.05	0.98	0.0001	0.002703
0.76	0.71	2.97	1.16	0.96	5.1076	1.71	0.76	0.21	0.11	0.98	0.0004	0.00548
1.15	1.12	1.99	0.77	0.94	0.7569	0.38	1.19	0.0613	0.086	0.99	0.0049	0.004118
1.52	1.42	1.39	1.16	0.95	0.0009	0.000647	1.54	0.0673	0.13	0.99	0.0144	0.009351

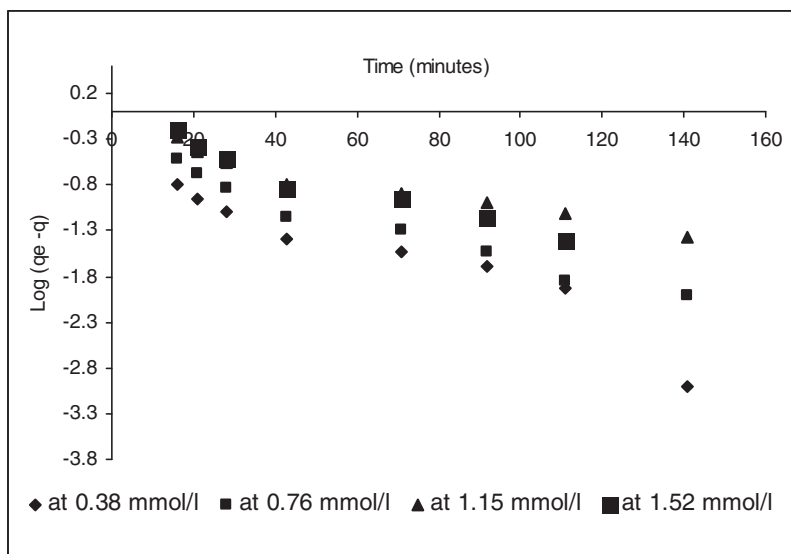


Fig. 10. Study of Pseudo-first-order model at 298K in concentration range of 0.38–1.52 mmol⁻¹, and 150 rpm.

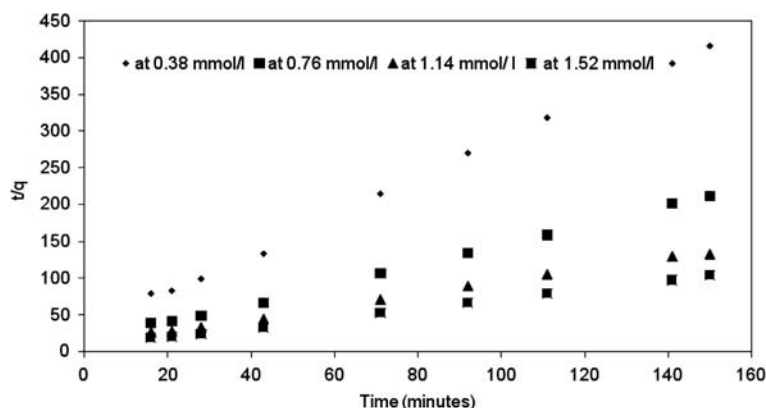


Fig. 11. Study of pseudo-second-order model at 298 K in concentration range of 0.38–1.52 mmol⁻¹, and at 150 rpm.

Eqs. (18) and (19) represent the relations for film and pore diffusion [67].

$$D_f = 0.23 \left[\frac{R_p \varepsilon}{t^{1/2}} \times \frac{q_e}{C_0} \right] \tag{18}$$

$$D_p = 0.03 \left[\frac{R_p}{t^{1/2}} \right] \tag{19}$$

where D_p and the D_f are diffusion coefficients (cm²s⁻¹), R_p =radius of the adsorbate particle=0.0025 cm, and ε =thickness of the film=10⁻³ cm [68], $t^{1/2}$ =half of the time required for total biosorption. If the adsorbate ion sorption onto the surface of

adsorbent is a film diffusion-controlled phenomena, the value of D_f lies in the range of 10⁻⁶–10⁻⁸ cm²s⁻¹, and if the metal ion adsorption rate is determined by pore diffusion, the value of D_p lies in the range of 10⁻¹¹–10⁻¹³ cm²s⁻¹. Both the equations of diffusivity assume the particle shape as dimensionally spherical. Both diffusion coefficients were evaluated and the results indicated the answer of diffusion coefficients much proficiently in the range of film diffusion, i.e. $D_f=7.16 \times 10^{-6}$ cm²s⁻¹ rather than in stipulations of pore diffusion, i.e. $D_p=8.33 \times 10^{-6}$ cm²s⁻¹. Gupta et al. [66] sorted out the biosorption of Cr (VI) onto surface of raw and acid-treated algae and reported that the film diffusion value came in the range of 10⁻⁶ cm²s⁻¹, signifying the ascendancy of film diffu-

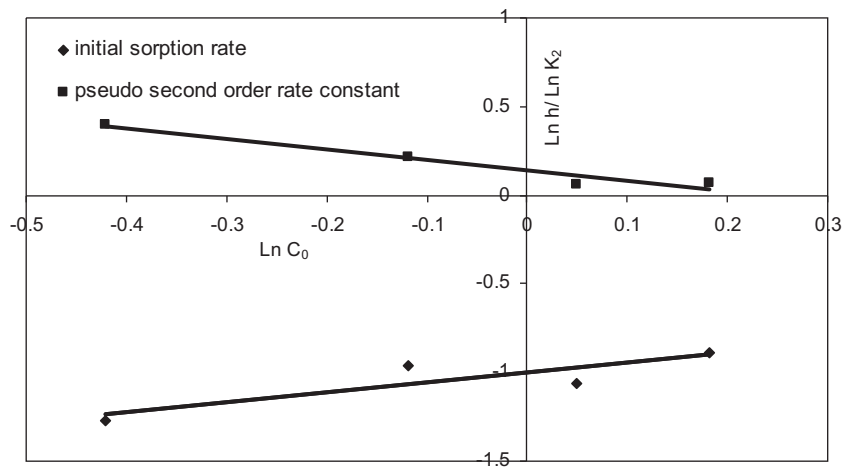


Fig. 12. Plot of initial sorption constant ($\text{mmol}^{-1}\text{g}^{-1}\text{min}^{-1}$) and reaction constant (K_2 , $\text{g mmol}^{-1}\text{min}^{-1}$) V_s initial concentration of Zn(II) ion at 298 K, 150 rpm, and pH=5.

Table 3
Study of intraparticle model and Bangham’s model in the concentration range of 0.38–1.52 mmol l^{-1} , 298 K, 150 rpm and at pH 5

Metal ion concentration (mmol l^{-1})	Intraparticle diffusion model		Bangham’s model	
	K_{id} ($\text{mol g}^{-1}\text{min}^{-0.5}$)	R^2	K_0	R^2
0.38	0.016	0.83	11.61	0.95
0.76	0.03	0.80	10.34	0.93
1.15	0.05	0.85	13.09	0.94
1.52	0.06	0.82	11.12	0.94

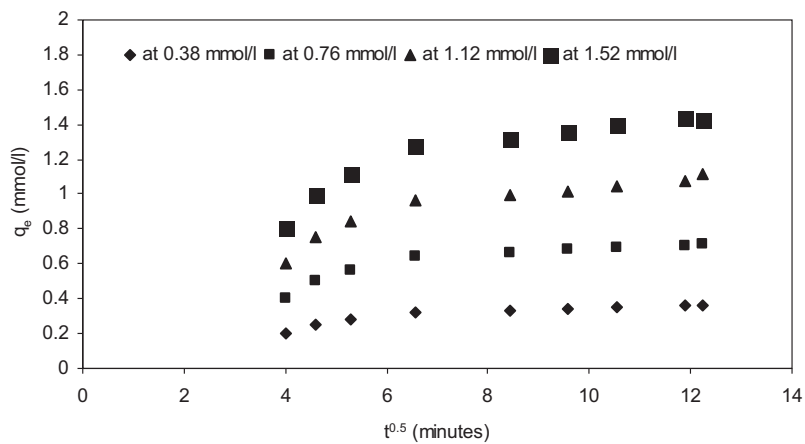


Fig. 13. Study of intraparticle model at 298K in range of 0.38–1.52 mmol l^{-1} adsorbate concentration, 150 rpm, and adsorbent dose 1 g l^{-1} .

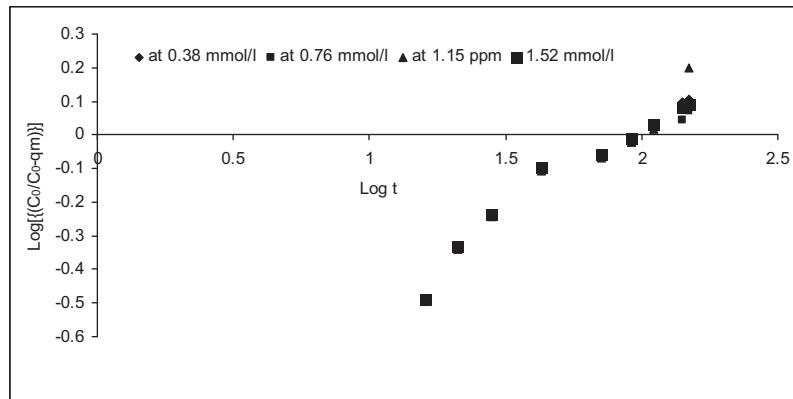


Fig. 14. Study of Bangham’s model at 298 K, 0.38–1.52 mmol⁻¹ Zn(II) ion concentration.

sion in case of metal ions adsorption onto living and nonliving biomass surface.

3.8. Thermodynamic modeling

Thermodynamic studies in metal biosorption system are very crucial to delineate the feasibility of the system as spontaneous or nonspontaneous schematically [35,36,69]. Gibbs free energy (ΔG , kJ/mol) of the system measures the degree of spontaneity. Thermodynamic feasibility of Zn(II) ion sorption onto the surface of ACEUB was predicted in terms of Gibbs free energy (ΔG kJ/mol), Entropy (ΔS , kJ/molK), and Enthalpy (ΔH , kJ/mol). Eqs. (20)–(22) were used to compute the above-mentioned parameters.

$$\Delta G = -RT \ln K_c \tag{20}$$

$$\ln K_c = \frac{\Delta S}{R} - \frac{\Delta H}{RT} \tag{21}$$

Hence,

$$K_c = \frac{C_a}{C_e} \tag{22}$$

where C_a (mg/l) is the Zn(II) ions adsorbed per liter, R =universal gas constant (8.314, J mol⁻¹ K⁻¹), T =absolute temperature, Kelvin, K_c =dimensionless, equilibrium constant.

Eq. (21) represents the straight-line equation cum relation between equilibrium constant and inverse of temperature. The plot extrapolated between $\ln K_c$ and $1/T$ yields the ΔG (from Eq. (20)), ΔH , and ΔS as intercept and slope of the plot, respectively. The results of Gibbs free energy, enthalpy, and entropy calculations are shown in Fig. 15 and Table 4.

$$\ln K_c = 4.1793/T - 12.946 \tag{23}$$

Eq. (23) represents the linear relation between equilibrium constant and temperature obtained through the plot extrapolated in between logarithmic

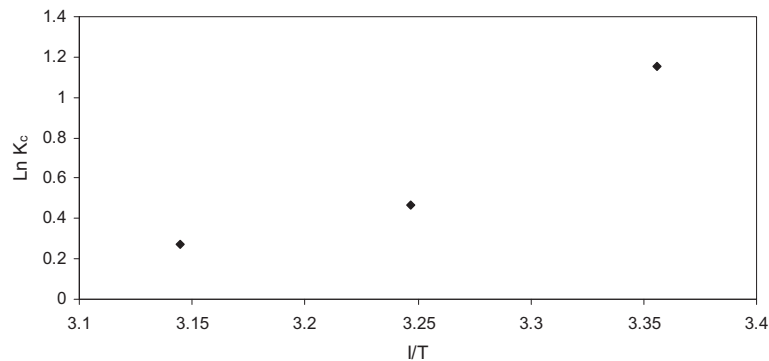


Fig. 15. Plot of equilibrium constant (K_c) and temperature ($1/T$).

Table 4
Study of Gibbs free energy as a function of various temperature gradients

Temperature (K)	ΔG (Gibbs free energy, kJ/mol)
298	−9,798
308	−1,702
318	−636

equilibrium constant and temperature. The values of enthalpy (ΔH) and entropy (ΔS) obtained from Eq. (24) were -34.74 (kJ mol^{-1}) and -107.63 ($\text{kJ mol}^{-1}\text{K}^{-1}$), respectively. The negative value of Gibbs free energy function (as shown in Table 4) demarcated the sorption of Zn(II) ion onto ACEUB surface was spontaneous reaction [30]. The value of Gibbs free energy increases with the increase in tem-

perature, which indicates that the Zn(II) ion sorption onto ACEUB surface was chemisorption rather than physical adsorption. Argun et al. [67] reported that the sorption of the Cd(II) and Pb(II) ion on the surface of activated pinecone was mediated by physical adsorption rather than metal ion binding mediated by chemical forces. The difference in the surface texture and surface chemistry between two activated carbon derivatives would have made the difference in their sorption mechanisms. The negative values of enthalpy showed that process of Zn(II) ion sorption across liquid phase onto the surface of ACEUB was exothermic in nature together with negative entropy, which further indicated the reduced degree of randomness at the solid–liquid interface. Bligili [64] reported adsorption of the 4–chlorophenol onto surface of xad–four resins as endothermic reaction with reduced degree of randomness at the solid–liquid interface.

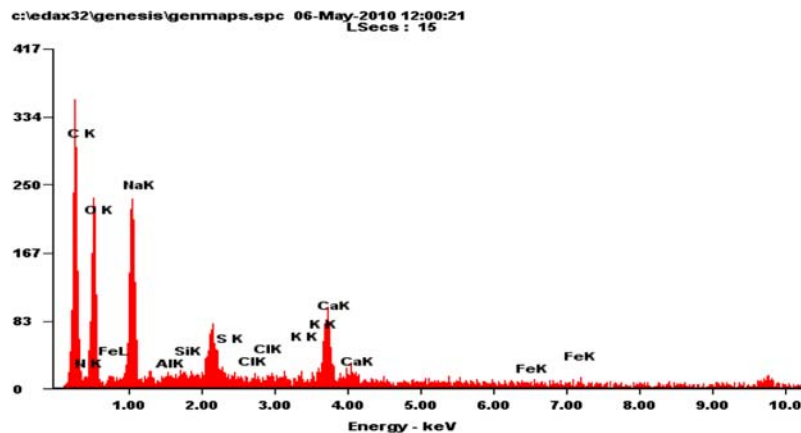


Fig. 16a. EDAX analysis of metal-unloaded base activated biomass.

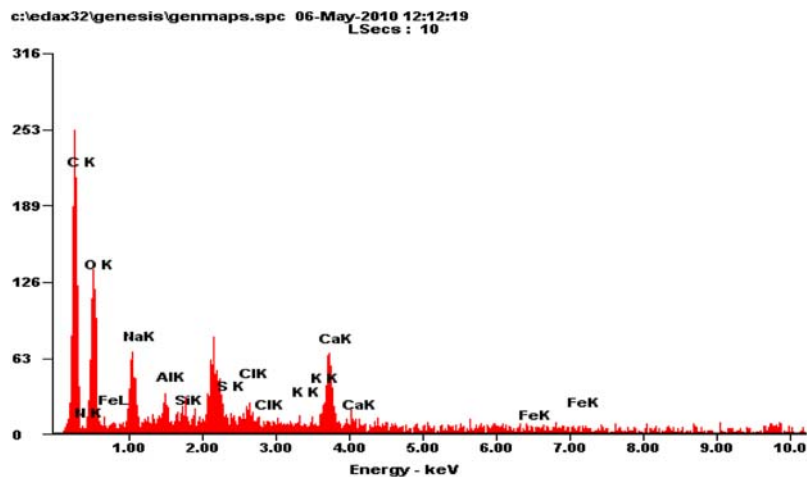


Fig. 16b. EDAX analysis of metal-loaded base activated biomass.

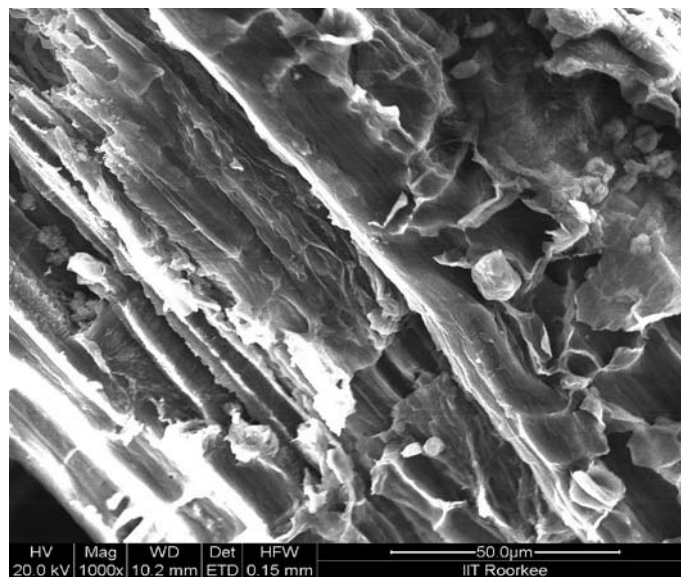


Fig. 17a. SEM photograph of base activated metal-unloaded biomass.

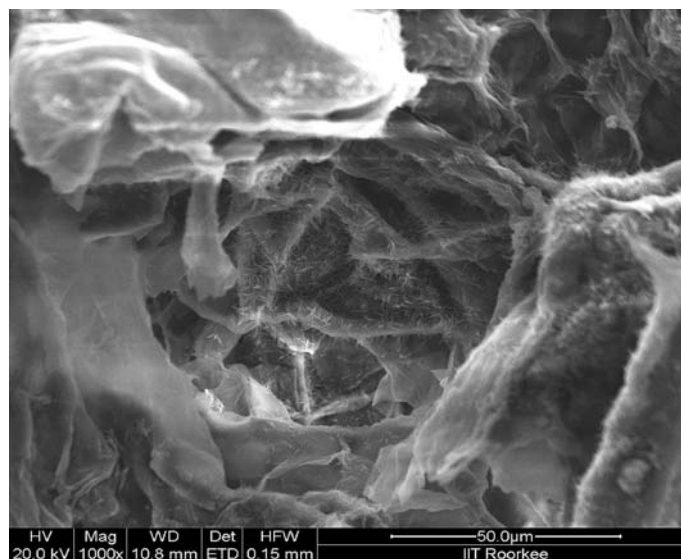


Fig. 17b. SEM photograph of base activated metal-loaded biomass.

3.9. Energy dispersive X-ray (EDAX) analysis

Figs. 16(a), 16(b), 17(a) and 17(b) represent the EDAX analysis and scanning electron micrograph of ACEUB before and after sorption of metal ion, respectively. Tables 5 and 6 have deduced the physicochemical characteristic of activated carbon before and after Zn(II) ion adsorption.

The EDAX analysis of both metal-unloaded and metal-loaded biomass represented in Figs. 17(a) and 17(b) unfolded the verity that the chemisorption type

of adsorption has occurred between Zn(II) ion present in liquid phase and active adsorptive sites present on the surface of activated carbon. The analysis of Table 4 and 5 together with the analysis of the Figs. 17(a) and 17(b) deduced the information that was radical decrease in the amount of sodium (Na^+) from 8.45 to 3.30%, before and after adsorption of Zn(II) onto activated carbon surface. In reality, these types of reactions belong to category of chemisorptive type of metal ion binding on adsorbent surface across liquid

Table 5
EDAX analysis of metal-unloaded base activated biomass

Element	Wt%	At%
CK	45.02	55.72
NK	4.32	4.58
OK	30.91	28.72
NaK	13.07	8.45
AlK	0.1	0.06
SiK	0.3	0.16
SK	0.3	0.14
ClK	0.09	0.04
KK	0.26	0.1
CaK	5.07	1.88
FeK	0.56	0.15
Matrix	Correction	ZAF

Table 6
EDAX analysis of metal-loaded base activated biomass

Element	Wt%	At%
CK	53.04	63.65
NK	2.43	2.5
OK	29.82	26.87
NaK	5.26	3.3
AlK	1.34	0.72
SiK	0.41	0.21
SK	0.47	0.21
ClK	0.92	0.37
KK	0.26	0.1
CaK	5.1	1.83
FeK	0.96	0.25
Matrix	Correction	ZAF

phase mediated by ion-exchange phenomenon. Vaghetti et al. [69] reported the chemisorption-mediated Cr(VI) ion removal from aqueous solutions by Brazilian pine fruit coat. Vaghetti et al. [69] made this conclusion based on the results obtained after desorption experiments, implementing acids, base and salt of various concentrations as desorbing agent. Furthermore, the scanning electron micrograph study discovered the information that activated carbon surface before sorption of Zn(II) ion was heterogeneous consisting a large number of pores and protrusions. The protrusions present on the surface of the ACEUB seemed to run inside the biomass cell matrix. The heterogeneous nature of metal-unloaded biomass indicated the tremendous cell surface area available to metal ion binding compared to metal-loaded biomass [52].

3.10. Ultimate and proximate analysis of raw eucalyptus bark EUB and ACEUB

The ultimate and proximate analysis of the raw eucalyptus bark (EUB) and ACEUB was carried out by using bomb calorimeter (Toshniwal electronics limited—Ajmer, India make), Muffle furnace (Wishwani Scientific traders and Instruments), and CHNS analyzer (CE-440 Elemental Analyzer, EAI Exter Analytical, Inc). These analyses decipher out the chemical composition of EUB and ACEUB.

The surface area of the biosorbent significantly affects the biosorption of heavy metal ion onto its surface. Greater is the surface area of the biosorbent, more is the opportunity for metal ions to bind. In the present work, the surface area of the EUB and ACEUB was measured by Micrometrics limited model ASAP 200 doped with the software ChemiSoft TPx V1.02.

Table 7
Physicochemical analysis of EUB and ACEUB

EUB	Carbon	Hydrogen	Sulfur	Nitrogen	Oxygen
<i>Ultimate analysis (%)</i>					
	54.95	3.5	0	0.02	41.52
ACEUB	Carbon	Hydrogen	Sulfur	Nitrogen	Oxygen
	65.54	2.14	0	0	32.32
<i>Proximate analysis (%)</i>					
	Volatile compounds	Fixed Carbon	Ash	Moisture	
EUB	35	39.1	21.3	4.6	
ACEUB	22.19	60.36	14.33	3.12	
Surface Area (BET) (m ² /g)					
EUB	28.37				
ACEUB	41.59				
Pore volume (m ³ /g)					
EUB	0.014				
ACEUB	0.02				

Table 8
Comparison of other biosorbent with ACEUB uptake capacity (mg g^{-1})

Biosorbent	Metal ion	Uptake capacity (mg g^{-1})	Reference
Bagasse based activated carbon	Zn(II)	31.1	[15]
Apricoat stones carbon	Zn(II)	13.21	[70]
Mango bark saw dust	Zn(II)	1.028	[7]
Pine apple peel powder	Zn(II)	0.45	[7]
Eucalyptus bark sawdust	Zn(II)	1.68	[7]
Red mud	Zn(II)	12.59	[71]
Thermal power plant ash	Zn(II)	5.75	[3]
Hazel nut	Zn(II)	1.95	[72]
Rice husk	Zn(II)	8.58	[44]
Bioslids	Zn(II)	36.66	[73]
<i>Spherothillus natans</i>	Zn(II)	3.4	[74]
<i>G. Thermoleovorans</i> Sub sp. <i>Strmboliensis</i>	Zn(II)	29	[75]
<i>Lamanaria japonica</i>	Zn(II)	91	[29]
<i>Goebacillus toebii</i> . Sub sp. <i>Decanicus</i>	Zn(II)	21.1	[75]
ACEUB	Zn(II)	92.83 ^a	This study

^a1.42 mmol g^{-1} of Zn(II) ion = 92.83 mg g^{-1}

The adsorption was carried out with the help of liquid nitrogen. The flow rate of the gas was kept 10 ml/min at standard temperature and pressure. Before the estimation of surface area, all the powdered biosorbent samples were dried at 373 K for 24 h to ensure the complete removal of moisture. Before and after the removal of moisture, the weight of the samples were measured by Electronic balance, model AW220, Shimadzu Corporation Japan. The ultimate and proximate analysis of the EUB and ACEUB is shown in Table 7.

It became evident from Table 7 that there were significant changes in the amount of carbon, hydrogen, nitrogen, and oxygen between the activated carbons. Furthermore, the values BET surface area and pore volume were higher in the case of ACEUB compared to EUB. The variation in the values of BET surface area, pore volumes, carbon, hydrogen, nitrogen, oxygen, ash, moisture, fixed carbon, and volatile compounds between ACEUB and EUB was due to the modifications on the surface of sawdust due to the alkaline treatment resulting in an increase in the surface area, pore volume, and pore diameter [22].

Table 8 represents the comparative analysis of sorption capacities various biosorbents utilized in other research investigations against the present study.

Zn(II) ion uptake by ACEUB as established in present investigation through batch experiments was compared with the uptake capacity of other adsorbents cited in other research work (Table 6). Although data represented in Table 8 would have been derived in different environmental conditions and adsorption

mechanisms, it still provides significant information of biosorbent selection for mass-scale continuous industrial operations.

5. Conclusion

Plant biomass activation was mediated by 0.2 M NaOH followed by thermal activation at 1,123 K. The maximum percentage removal of Zn(II) ion and Zn(II) ion uptake capacity were 93.42% and 1.42 mmol g^{-1} (92.83 mg g^{-1}) obtained, respectively, at equilibrium. Isotherm modeling of the data obtained at fixed temperature and at various concentrations (0.38–1.52 mmol l^{-1}) together with dynamic modeling indicated the ascendancy of Freundlich isotherm with pseudo-second-order model against Langmuir isotherm and pseudo-first-order reaction kinetics. Intraparticle diffusion and Bangham's model were validated along with the evaluation of diffusivity coefficients, and the results obtained indicated the supremacy of film diffusion over intraparticle diffusion. The thermodynamic studies of Zn(II) ion sorption over activated carbon surface across liquid phase yielded ΔG (–9,798 to –636 kJ mol^{-1}), ΔH (–34.74 kJ mol^{-1}), and ΔS (–107.63 $\text{kJ mol}^{-1} \text{K}^{-1}$), respectively. The negative sign with all the thermodynamic parameters categorized the Zn(II) binding on activated carbon surface as spontaneous, exothermic with decreased rate of entropy at solid and liquid phase at higher temperature gradient. The values obtained in ultimate, proximate, BET surface area,

pore volume, and pore size analysis showed the physicochemical difference between EUB and ACEUB.

References

- [1] J. Febranto, A.N. Kosasih, J. Sunarso, Y.H. Ju, N. Indraswati, S. Ismadji, Equilibrium and kinetic studies in adsorption of heavy metals using biosorbent: A summary of recent studies, *J. Hazard. Mater.* 162 (2009) 616–645.
- [2] P. Suksabye, A. Nakajima, P. Thiravetyan, Y. Baba, W. Nakanpote, Mechanism of Cr (VI) adsorption by coir pith studied by ESR and adsorption kinetic, *J. Hazard. Mater.* 161 (2009) 1103–1108.
- [3] L. Tofan, C. Padararu, D. Bilba, M. Rotariu, Thermal power plant ash as sorbent for the removal of Cu(II) and Zn(II) ions from wastewaters, *J. Hazard. Mater.* 156 (2008) 1–8.
- [4] H. Arslanoglu, H.S. Altundogan, F. Tumen, Heavy metals binding properties of esterified lemon, *J. Hazard. Mater.* 164 (2009) 1406–1413.
- [5] W. Shen, S. Chen, S. Shi, X. Li, X. Zhang, W. Hu, H. Wang, Adsorption of Cu(II) and Pb(II) onto diethylenetriamine–bacterial cellulose, *Carbohydr. Polym.* 75 (2009) 110–114.
- [6] V.K. Gupta, A. Rastogi, Biosorption of hexavalent chromium by raw and acid treated green alga *Oedogonium hatei* from aqueous solutions, *J. Hazard. Mater.* 163 (2009) 396–402.
- [7] V. Mishra, C.B. Majumder, V.K. Agarwal, Biosorption of Zn (II) onto surface of non living Biomasses: A comparative Study of Adsorbent Particle size and removal capacity of three different biomasses, *Water Air Soil Pollut.* 211 (2009) 489–500.
- [8] M.T. Alvarez, C. Crespo, B. Mattiason, Precipitation of Zn(II), Cu(II) and Pb(II) at bench scale using biogenic sulphide from utilization of volatile fatty acids, *Chemosphere* 66 (2007) 1667–1683.
- [9] A. Grzeszczyk, M.R. Rosocka, Extraction of zinc (II), iron (II) and iron (III) from chloride with dibutylbutylphosphonate, *Hydrometallurgy* 86 (2007) 72–79.
- [10] G. Csicsovszki, T. Kekesi, T.I. Torok, Selective recovery of Zn and Fe from spent pickling acid solutions by the combination of anion exchange and membrane electrowinning technique, *Hydrometallurgy* 77 (2007) 19–28.
- [11] J.A. Carrera, E. Bringas, M.F.S. Roman, I. Ortiz, Selective membrane alternative to the recovery of zinc from hot dip galvanizing effluents, *J. Membr. Sci.* 326 (2009) 672–680.
- [12] C.A. Basha, S.J. Selvi, E. Ramasamy, S. Chellammal, Removal of arsenic and sulphate from the copper smelting industrial effluent, *Chem. Eng. J.* 141 (2008) 89–98.
- [13] M.B. Mansur, S.D.F. Rocha, F.S. Magalhaes, J.D.S. Benedetto, Selective extraction of Zn(II) over Fe(II) from spent hydrochloric acid pickling effluents by liquid–liquid extraction, *J. Hazard. Mater.* 150 (2008) 669–678.
- [14] R.R. Sheha, Sorption behavior of Zn(II) ions on synthesized hydroxyapatites, *J. Colloid Interface Sci.* 310 (2007) 18–26.
- [15] D. Mohan, P.K. Singh, Single and multi component adsorption of cadmium and zinc using activated carbon derived from bagasse—an agricultural waste, *Water Res.* 36 (2002) 2304–2318.
- [16] V.C. Srivastava, I.D. Mall, I.M. Mishra, Adsorption thermodynamics and isosteric heat of toxic metal ion onto bagasse fly ash (BFA) and rice husk ash (RHA), *Chem. Eng. J.* 132 (2007) 267–278.
- [17] C.J. Klein, Zinc supplementation, *J. Am. Diet Assoc.* 100 (2000) 1137–1142.
- [18] A.R. Iftikhar, H.N. Bhatti, M.A. Hanif, R. Nadeem, Kinetic and thermodynamic aspects of Cu(II) and Cr(III) removal from aqueous solutions using rose waste biomass, *J. Hazard. Mater.* 161 (2009) 941–947.
- [19] C.E.M. Romain, E. Pinelli, B. Porrut, J. Silvestre, M. Guiesse, Assessment of genotoxicity of Cu and Zn in raw and anaerobically digested slurry with *Vicia faba* micronucleus test, *Mutat. Res.* 672 (2009) 113–118.
- [20] I.A. Sengil, M. Ozacar, Competitive biosorption of Pb²⁺, Cu²⁺ and Zn²⁺ ions from aqueous solutions onto valonia tannin resin, *J. Hazard. Mater.* 166 (2009) 1488–1494.
- [21] M. Arshad, M.N. Zafar, S. Younis, R. Nadeem, The use of Neem biomass for the biosorption of zinc from aqueous solutions, *J. Hazard. Mater.* 157 (2008) 534–540.
- [22] W.S.W. Nagh, M.A.K.M. Hanfiah, Removal of heavy metals ions from wastewaters by chemically modified plant waste as adsorbents: A review, *Bioresour. Technol.* 99 (2008) 3935–3948.
- [23] L. Agouborde, R. Nazia, Heavy metals retention capacity of a nonconventional sorbents developed from a mixture industrial and agricultural waste, *J. Hazard. Mater.* 167 (2009) 536–544.
- [24] A.B.P. Marin, J.F. Orunto, M.I. Aguilar, V.F. Meseguer, J.F. Saez, M. Llorens, Use of chemical modification to determine the binding of Cd(II), Zn(II) and Cr(III) ions by orange waste, *Biochem. Eng. J.* 53 (2009) 2–6.
- [25] T.K. Naiya, P. Chowdhury, A.K. Battacharya, S.K. Das, Sawdust and neem bark as low cost natural biosorbent for adsorptive removal of Zn(II) and Cd(II) ions from aqueous solutions, *Chem. Eng. J.* 148 (2009) 68–79.
- [26] F. Kaczla, M. Marques, W. Hogland, Lead and vanadium removal from a real industrial waste water by gravitational settling/sedimentation and sorption onto *Pinus sylvestris* sawdust, *Bioresour. Technol.* 100 (2009) 235–243.
- [27] V.B.H. Dang, H.D. Doan, T. Dang-Vu, A. Lohi, Equilibrium and kinetics of biosorption of cadmium (II) and copper (II) ions by wheat straw, *Bioresour. Technol.* 100 (2009) 211–219.
- [28] T. Fan, Y. Liu, B. Feng, G. Zeng, C. Yang, M. Zhou, H. Zhou, Z. Tan, X. Wang, Biosorption of cadmium (II), zinc (II) and lead (II) by *Penicillium simplicissimum*: Isotherms, kinetics and thermodynamics, *J. Hazard. Mater.* 160 (2008) 655–661.
- [29] T.A. Davis, B. Volesky, A. Mucci, A review on biochemistry of heavy metal biosorption by brown algae, *Water Res.* 37 (2003) 4311–4330.
- [30] Y. Khambhaty, K. Mody, S. Basha, B. Jha, Kinetics, Equilibrium and thermodynamic studies on biosorption of hexavalent chromium by dead fungal biomass of marine *Aspergillus niger*, *Chem. Eng. J.* 145 (2009) 489–495.
- [31] L. Velasquez, J. Dussan, Biosorption and bioaccumulation of heavy metals on dead and living biomass of *Bacillus Sphaericus*, *J. Hazard. Mater.* 167 (2009) 713–716.
- [32] T.K. Budinova, K.M. Gergova, N.V. Petrov, V.N. Minkova, Removal of metal ions from aqueous solutions by activated carbon obtained from different raw materials, *J. Chem. Technol. Biotechnol.* 60 (1994) 177–182.
- [33] M.A.F. Gracia, J.R. Ultrilla, J.R. Gorduillio, T. Bautista, Adsorption of zinc, cadmium and copper on activated carbons obtained from agricultural by products, *Carbon* 26 (1988) 363–373.
- [34] H. Arslanoglu, H.S. Altundogan, F. Tumen, Heavy metals binding properties of esterified lemon, *J. Hazmat. Mater.* 164 (2009) 713–716.
- [35] V. Sarin, K.K. Pant, Removal of chromium from industrial waste by using eucalyptus bark, *Bioresour. Technol.* 97 (2006) 15–20.
- [36] V. Sarin, T. Singh, K.K. Pant, Thermodynamic and breakthrough column studies for selective sorption of chromium from industrial effluents on activated eucalyptus bark, *Bioresour. Technol.* 97 (2006) 1986–1993.
- [37] I. Ghodbane, L. Nouri, O. Hamdaoui, M. Chiha, Kinetic and equilibrium study for the sorption of cadmium (II) ions from aqueous phase by eucalyptus bark, *J. Hazmat. Mater.* 152 (2008) 148–158.

- [38] H.I. Li, J.L. Madden, Analysis of leaf oils from a eucalyptus species trial, *Biochem. Syst. Ecol.* 23 (1995) 167–177.
- [39] M. Yatagi, T. Takashi, Successive extractives of *eucalyptus* essential oils and successive extractives of *eucalyptus* leaves, *Biomass* 4 (1984) 305–310.
- [40] A. Celekli, M. Yavuzatmaca, H. Bozkurt, Kinetics and equilibrium studies on the adsorption of reactive red 120 from aqueous solution on *Spirogyra majuscula*, *Chem. Eng. J.* 152 (2009) 139–145.
- [41] N.Y. Mezenner, A. Bensmaili, Kinetics and thermodynamic study of phosphate adsorption on iron–hydroxide eggshell waste, *Chem. Eng. J.* 147 (2009) 87–96.
- [42] Y. Nughlou, E. Malock, Thermodynamic and kinetic studies for environmental friendly Ni(II) biosorption using waste pomace of olive oil factory, *Bioresour. Technol.* 100 (2009) 2357–2380.
- [43] R.R. Dash, C.B. Majumder, A. Kumar, Removal of cyanide from waste and wastewater using granular activated carbon, *Chem. Eng. J.* 146 (2009) 408–413.
- [44] C.G. Rocha, D.A.M. Zaia, R.V.S. Alfaya, A.A.S. Alfaya, Use of rice straw as biosorbent for removal of Cu(II), Zn(II), Cd(II) and Hg(II) ions in industrial effluents, *J. Hazard. Mater.* 166 (2009) 383–388.
- [45] B. Bayat, Combined removal of zinc (II) and cadmium (II) from aqueous solutions by adsorption onto high calcium Turkish fly ash, *Water Air Soil Pollut.* 136 (2002) 66–92.
- [46] A. Scotti, S. Silva, C. Baffi, Effect of fly ash pH on the uptake of heavy metals by chicory, *Water Air Soil Pollut.* 109 (1999) 397–409.
- [47] A. Akil, M. Mouflih, S. Sebti, Removal of heavy metal ions from water by using calcined phosphate as a new adsorbent, *J. Hazard. Mater.* 112 (2004) 183–190.
- [48] V.K. Gupta, I. Ali, Removal of lead and chromium from wastewater using bagasse fly ash—a sugar industry waste, *J. Colloid Interface Sci.* 271 (2004) 321–328.
- [49] V.K. Gupta, D. Mohan, S. Sharma, Removal of lead from wastewater using bagasse fly ash—a sugar industry waste material, *Sep. Sci. Technol.* 33 (1998) 1331–1343.
- [50] Q. Feng, Q. Lin, F. Gong, S. Sugita, M. Shoya, Adsorption of lead and mercury by rice husk, *J. Colloid Interface Sci.* 274 (2004) 1–8.
- [51] A. Sari, M. Tuzen, Biosorption of total chromium from aqueous solution by red algae (*Ceramium virgatum*): Equilibrium, kinetic and thermodynamic studies, *J. Hazard. Mater.* 160 (2008) 349–355.
- [52] A. Ahmad, M. Rafatullah, O. Sulaiman, M.H. Ibrahim, Y.Y. Chii, B.M. Siddique, Removal of Cu(II) and Pb(II) ions from aqueous solutions by adsorption on sawdust of Meranti wood, *Desalination* 247 (2009) 636–646.
- [53] M. Riaz, R. Nadeem, M.A. Hanif, T.M. Ansari, K. Ur. Rehman, Pb(II) biosorption on hazardous aqueous streams using *Gossypium hirsutum* (cotton) waste biomass, *J. Hazard. Mater.* 161 (2009) 88–94.
- [54] R.R. Dash, C.B. Majumder, A. Kumar, Treatment of metal cyanide bearing waste water by simultaneous adsorption and biodegradation (SAB), *J. Hazard. Mater.* 152 (2008) 387–396.
- [55] R. Nadeem, T.M. Ansari, K. Akhtar, A.M. Khalid, Pb(II) sorption by pyrolysed *Pongamia pinnata* pods carbon (PPPC), *Chem. Eng. J.* 152 (2009) 54–63.
- [56] W.T. Tsai, J.M. Yang, C.W. Lai, Y.H. Cheng, C.C. Lin, C.W. Yeh, Characterization and adsorption properties of eggshell and egg shell membrane, *Bioresour. Technol.* 97 (2006) 488–493.
- [57] Meatcafe and Eddy, *Wastewater Engineering, Treatment and Reuse*, Tata Mc Hill, New Delhi, 2003.
- [58] Y. Liu, Y.J. Liu, Biosorption isotherms, kinetics and thermodynamics, *Sep. Sci. Purif. Technol.* 61 (2008) 229–242.
- [59] M. Ozacar, I.A. Sengil, A kinetic study of metal complex dye sorption onto pine sawdust, *Process Biochem.* 40 (2005) 562–572.
- [60] S. Basha, Z.V.P. Murthy, B. Jha, Sorption of Hg(II) onto *Carica papaya*: Experimental studies and design of batch sorber, *Chem. Eng. J.* 147 (2009) 226–234.
- [61] K.V. Kumar, K. Ramamurthi, S. Sivanesan, Modeling the mechanism involved during sorption of methylene blue onto fly ash, *J. Colloid Interface Sci.* 284 (2005) 14–21.
- [62] Y.S. Ho, G. McKay, The kinetics of sorption of basic dyes from aqueous solutions by sphagnum moss peat, *Can. J. Chem. Eng.* 76 (1988) 822–827.
- [63] A.E. Nemr, Potential of Pomegranate husk carbon for Cr (VI) removal from wastewater: Kinetic and isotherms studies, *J. Hazard. Mater.* 161 (2009) 132–141.
- [64] M.S. Bligili, Adsorption of 4–chlorophenol aqueous solutions by xad–4 resin: Isotherm, kinetic, and thermodynamic analysis, *J. Hazard. Mater. B* 137 (2006) 157–164.
- [65] Q. Sun, L. Yang, Adsorption of basic dyes from aqueous solutions onto modified peat resin, *Water Res.* 37 (2003) 1535–1544.
- [66] V.K. Gupta, A. Rastogi, Biosorption of hexavalent chromium by raw and acid treated algae *Oedogonium hatie* from aqueous solutions, *J. Hazard. Mater.* 163 (2009) 396–402.
- [67] M.E. Argun, S. Dursun, M. Karatas, M. Guru, Activation of pine cone using Fenton oxidation for Cd(II) and Pb(II) removal, *Bioresour. Technol.* 99 (2008) 8691–8698.
- [68] K.G. Varshney, A.A. Khan, U. Gupta, S.M. Maheshwari, Kinetics of adsorption of phosphamidon on antimony (V) phosphate cation exchanger: Evaluation of the order of reaction and some physical parameters, *Colloid Surface A: Physiochem. Eng. Asp.* 113 (1996) 19–23.
- [69] J.C.P. Vaghetti, E.C. Lima, B. Royer, J.L. Brasil, B.M.D. Cunha, N.M. Simon, N.F. Cardoso, C.P.Z. Norena, Application of Brazilian–pine fruit coat as a biosorbent to removal of Cr (VI) from aqueous solutions—kinetics and equilibrium study, *Biochem. Eng. J.* 42 (2008) 67–76.
- [70] T.K. Budinova, K.M. Gergova, N.V. Petrov, V.N. Vinkova, Removal of metals from aqueous solutions by activated carbons derived from different raw materials, *J. Chem. Biotechnol.* 60 (1994) 177–182.
- [71] E. Lopez, B. Soto, M. Arias, A. Nunez, D. Rubinos, M.T. Barral, Adsorbent particle of red mud and its use for wastewater treatment, *Water Res.* 3 (1998) 1314–1322.
- [72] G. Cimino, A. Passerini, G. Toscano, Removal of toxic cations and Cr (VI) from aqueous solutions by hazelnut, *Water Res.* 34 (2000) 2955–2962.
- [73] L. Norton, K. Baskaran, T. McKenzie, Biosorption of zinc from aqueous solutions using biosolids, *Adv. Environ. Res.* 8 (2004) 629–635.
- [74] A. Lodi, C. Solisio, A. Converti, D.M. Borghi, Cadmium, Zinc, copper, silver, chromium (III) removal from wastewater by *Sphaerotillus natans*, *Bioprocess Eng.* 19 (1998) 197–203.
- [75] S. Ozdemir, E. Kilinc, A. Poli, B. Nicolaus, K. Guven, Biosorption of Cd, Cu, Ni, Mn and Zn from aqueous solutions by thermophilic bacteria, *Geobacillus toebii* sub sp. *stromboliensis* sub. sp. *decanicus* and *Geobacillus thermoleovorans* sub. sp. *Stromboliensis*: Equilibrium, kinetic and thermodynamic studies, *Chem. Eng. J.* 152 (2009) 195–206.